

# Scanning Kelvin probe and photoemission electron microscopy of organic source-drain structures

K. Müller<sup>a,\*</sup>, A. Goryachko<sup>a</sup>, Y. Burkov<sup>a</sup>, C. Schwiertz<sup>a</sup>,  
M. Ratzke<sup>b</sup>, J. Köble<sup>c</sup>, J. Reif<sup>b</sup>, D. Schmeißer<sup>a</sup>

<sup>a</sup> Brandenburgisch Technische Universität Cottbus, Angewandte Physik-Sensorik,  
P.O. Box 101344, 03013 Cottbus, Germany

<sup>b</sup> Brandenburgisch Technische Universität Cottbus, Experimentalphysik-Materialwissenschaften,  
P.O. Box 101344, 03013 Cottbus, Germany

<sup>c</sup> Omikron NanoTechnology GmbH, 65232 Taunusstein, Germany

Available online 29 September 2004

## Abstract

In order to optimize organic field effect transistors (OFETs), the characterisation of active-layer surfaces in terms of their roughness, chemical composition and distribution of surface potentials is important. We report on high-resolution microscopic mapping of organic source-drain structures with P3HT as the semiconductor by scanning Kelvin probe microscopy (SKPM) and photoemission electron microscopy (PEEM). It was shown that PEEM is able to characterise the surface morphology (roughness), the chemical homogeneity and the composition of organic structures. The two-dimensional mapping of surface potentials by SKPM with applied source-drain voltages is shown to be an important ingredient of OFETs failure mode analysis.

© 2004 Elsevier B.V. All rights reserved.

**Keywords:** Photoemission electron microscopy (PEEM); Scanning Kelvin probe microscopy (SKPM); OFET

## 1. Introduction

An important ingredient for optimizing the performance of organic thin-film transistors is characterisation of their active layers with high spatial resolution. These studies need to be performed in terms of surface and interlayer potentials or the chemical and morphological homogeneity of the layers. For example, the roughness of the isolation layer leads to a reduced field effect mobility of the active layer due to inhomogeneous or incomplete accumulation layer. High roughness of electrodes leads to an increased effective contact area between the semiconductor and the drain electrode, resulting in a higher amount of injected electrons. A higher effective contact area should be equivalent to a thicker semiconducting layer, leading to an increased rate of injected electrons and consequently insufficient saturation of the transistor [1].

The scanning Kelvin probe microscopy (SKPM) was successfully applied for studies of inorganic semiconductor structures like solar cells in terms of a workfunction contrast [2]. High-resolution characterisation of surface potentials in organic transistors using SKPM was first described by Sirringhaus et al. [3]. An ideal system with Au electrodes and SiO<sub>2</sub>/Si for isolation and bottom gate was used for studies with regioregular poly(3-hexylthiophene) (P3HT) as the active layer. It was shown that SKPM reflects the electrostatic potential of the accumulation layer at the P3HT/SiO<sub>2</sub> interface. Still not ideal but full organic structures also need to be studied in laterally within the device plane. In this contribution we used SKPM for studying profiles and two-dimensional maps of the surface potential in the channel region of organic source-drain structures with applied voltage.

Generally SKPM gives information depending on the value  $\varphi = \varphi(x) + \Delta\phi(x)$ , where  $\Delta\phi(x)$  is the difference in work function between the sample and the tip and  $\varphi(x)$  is the local electric potential [3].  $\varphi(x)$  itself gives information on

\* Corresponding author. Tel.: +49 355 694067; fax: +49 355 693931.  
E-mail address: [muellerk@tu-cottbus.de](mailto:muellerk@tu-cottbus.de) (K. Müller).

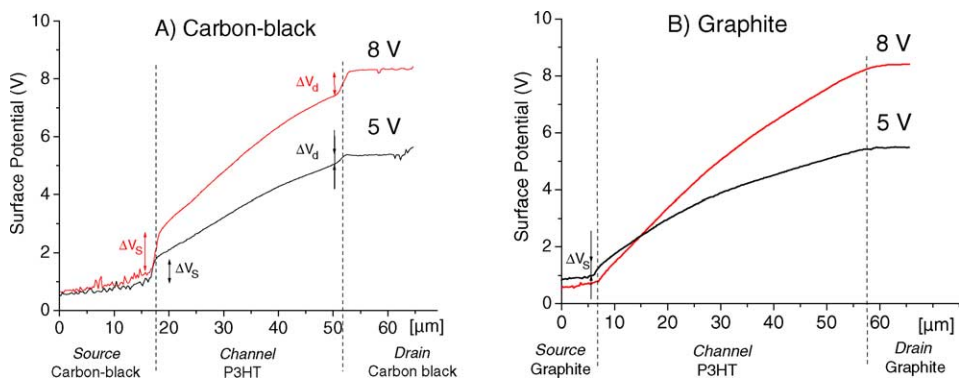


Fig. 1. Potential profiles of source-drain structures at applied source-drain voltage, measurements performed in ambient air. (A) Carbon black; (B) colloidal graphite.

additional surface charges due to the applied fields, gradients or inhomogeneities of the local source-drain field or additional potential distributions due to an applied gate voltage.

In addition, we used photoemission electron microscopy (PEEM) to introduce it as complementary method for our measurements of the differences in surface potentials. It was shown that excitation with a standard Hg lamp results in useful resolution and sufficient signal intensity when using electrostatic lenses as imaging system for photoelectrons [4,5]. Generally the contrast of PEEM images is of electron yield, bright areas represent regions with higher electron emission. The rate of electron yield is influenced by topography (shadowing), work function (different materials or doping levels, reduced work function at edges), or chemical inhomogeneities, resulting in a different yield rate [6]. With these two independent methods, namely SKPM and PEEM, the OFETs characterisation results can be cross-checked and failure mode analysis conclusions supplemented. In addition, a separation of work function from the morphology dependent surface potentials or lateral distributions should be possible.

## 2. Experimental

The experiments presented in this contribution were performed on source-drain structures with spin-coated regioregular poly(3-hexylthiophene) (P3HT) as semiconducting layer, about 100 nm in thickness. The structures themselves are made of organic materials: plain printing foil for water soluble ink as substrate and the source and drain electrodes were plotted with a computer-driven plotter (Rolland DXY-1150A). We used two types of conducting organic material. A: colloidal graphite (Plano W. Planet) diluted in water and homogenised in an ultrasonic bath and B: carbon black for ink jet printing with an average grain size of about 20 nm (Degussa, type AN1-25/L) and glycol as ink additive. With this procedure we were able to plot structures in high resolution (S/D-distance  $20 \pm 10 \mu\text{m}$ ) without any additional preparation of the substrate. By taking this method and with an additional spin-coated layer of PMMA, solved in ethylac-

etate, we are able to produce transistor structures in top- and bottom-gate performance [7].

The distribution of electrical potential on the surface was measured with SKPM technique, using the Omicron VT atomic force microscope (AFM) in ultra-high vacuum (UHV) environment and the NT-MDT Smena AFM in ambient environment. Both instruments operated in the basic non-contact AFM mode, but used different schemes to extract the Kelvin signal. The UHV AFM utilized a single pass technique, meaning, that surface topography was acquired simultaneously with surface potential distribution, the later using the frequency modulation (FM) technique [2]. The ambient AFM was operated in the dual pass mode, meaning, that each line in the raster was scanned twice. During the first pass, topography was obtained in the usual non-contact AFM mode, and after completing a line and digitally storing its topography  $z(r)$ , the tip was elevated 100 nm above the first pass trajectory and moved along the trajectory  $z(r) + 100 \text{ nm}$ . During this second pass the surface potential was acquired using the amplitude modulation (AM) technique [2].

For our PEEM measurements, we used radiation of a standard high-pressure Hg lamp (4.9 eV). The PEEM optics is an adapted OMICRON FOCUS-IS-PEEM with a CCD camera and a simulated hemispherical analyser [5,8]. The samples used for these measurements were partially spin-coated with P3HT to compare the contrast in workfunction of areas with and without a covering of P3HT. Around the measured area, the surface of the samples was again covered with graphite to prevent charging processes.

## 3. Results and discussion

### 3.1. SKPM measurements in ambient air

In this section we report on the results of SKPM measurements on source-channel-drain structures with P3HT semiconductor with voltage applied between source and drain, but without gate dielectric and gate electrode. Fig. 1 shows potential profiles of two source-channel-drain structures with

Table 1  
Potential drops at the interfaces

Electrode material	$\Delta V_d$	$\Delta V_s$	Applied voltage
Carbon black	1.0	0.3	5
	1.5	1.0	8
Graphite	0	0	5
	0.3	0	8

graphite and carbon black electrodes at different source-drain voltages, namely 5 and 8 V obtained in ambient air. The lateral resolution of the potential profile is in the range of 200 nm, as revealed by smallest potential features on top of the electrodes.

Marked features of the profiles in Fig. 1 are the abrupt potential drops  $\Delta V_d$  at drain and  $\Delta V_s$  at source at the electrode/P3HT interface (Fig. 1A), summarised in Table 1. Inside the channel between the two carbon black electrodes the potential drop is linear with a small inhomogeneity in slope (Fig. 1A), in the case of graphite electrodes the potential drop in the channel has a more pronounced non-linearity. In smaller length scales, in the range of the above mentioned resolution of 200 nm, an additional superimposed heterogeneity was measured, here especially in the range of the carbon black source electrode, Fig. 1A. The value for this variation is in the order of 300 mV and not due to a signal noise of the SKPM. A better resolution of these fluctuations at the surface potential was measured in UHV, described later.

In conclusion, the information revealed by our SKPM measurements in air is split into three main scales or ranges with information on (i) the voltage drop at the interface electrode/polymer, (ii) linearity and (iii) fluctuations.

The voltage drop between the interface electrode semiconductor indicates a contact resistance due to different workfunctions of the two materials and makes it possible to characterise the quality of the measured contact. In larger scales, the measurement of potential gives information about the homogeneity of the transistor structure, especially the spin-coated P3HT layer and in consequence, the related transistor performance. The curvature observed in Fig. 1B could be caused by variations in thickness of the P3HT layer: a thicker layer

of the spin-coated semiconductor should generate a smaller potential drop. For a space charge as a result of charge injection we expect a reversed curvature corresponding to the  $x^{3/2}$ —law of the related potential distribution. A calibration procedure was performed to exclude non-linearities of the cantilever, but for further considerations we need a better statistics, compared with simulations of the potential distribution. Short-ranged information like the above mentioned heterogeneities in the carbon black electrode region should be due to a lateral distribution of a surface potential related to single grains or agglomerations of the carbon black particles, in this case.

The quality of the contact can be compared with the reported value for the contact resistance  $R_c = L(\Delta V_d + \Delta V_s)/I_{ds}$ , reported by Sirringhaus et al. [3] of a P3HT-Cr/Au structure, which is in a range of 50 k $\Omega$  cm. For our carbon black, we determined a value of about 10 k $\Omega$  cm for the two terminal devices used. The data measured by [3] are revealed for transistor structures with an applied gate voltage of  $-30$  V and with drain-source voltages in the linear (ohmic) regime ( $|U_{ds}|$  max. 8 V). The gate voltage causes an accumulation layer with approximately constant charge density in this range. In our measurements, the almost ohmic behaviour of the semiconductor was measured due to doping effects.

Next, we determined the workfunctions directly by taking UPS measurements under UHV conditions for the three different pure materials on an Fe substrate. We obtain the following values: Graphite, pure: 4.1 eV, Carbon black, pure: 3.8 eV and for P3HT, pure (thickness <500  $\mu$ m): 3.8 eV. This small difference of the workfunctions is related to the better adaptation of systems with carbon or graphite as source-drain electrodes in terms of the contact resistance. Differences between carbon black and colloidal graphite should be due to different ink additives (Graphite:  $\text{NH}_3$ , Carbon black: Glycol).

### 3.2. SKPM measurements in UHV

The following two-dimensional Kelvin characterisation was performed on a structure with source-drain electrodes

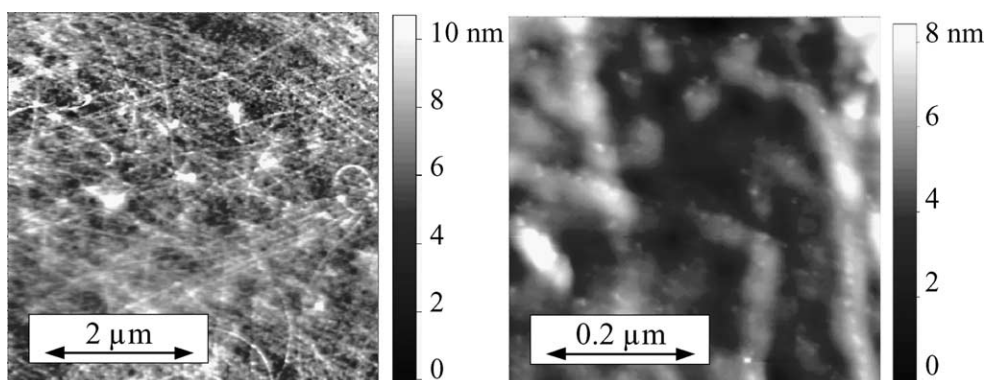


Fig. 2. UHV AFM images of the P3HT surface in the channel between the two carbon black electrodes.

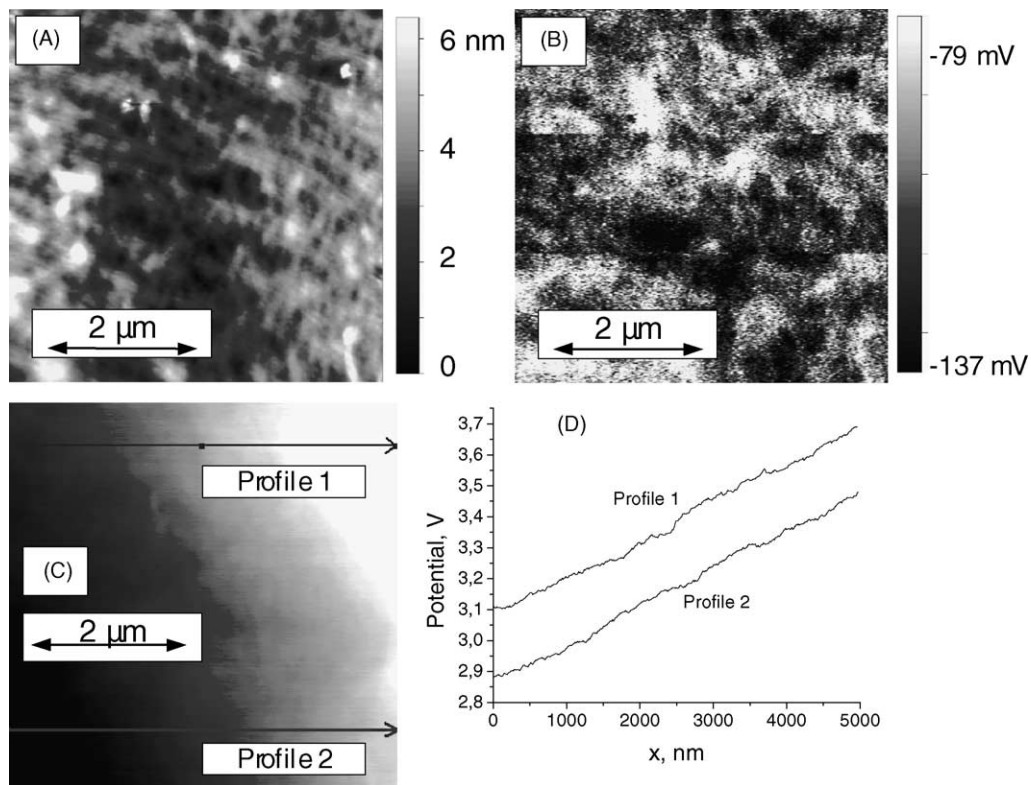


Fig. 3. (A) UHV AFM picture of the P3HT surface. (B) SKPM potential map without any applied source-drain voltage at the same position. (C) SKPM potential map at the same position with an applied source-drain voltage of 8 V. (D) Two potential profiles at different positions.

made of carbon black (Degussa) material. The channel of this structure was about  $60 \mu\text{m}$  in width, but the field of view in the Omicron VT AFM is only  $5 \mu\text{m} \times 5 \mu\text{m}$ . The potential profile needed to be composed of a sequence of images.

Fig. 2 shows two AFM images in topographic mode with  $5 \mu\text{m} \times 5 \mu\text{m}$  and  $1 \mu\text{m} \times 1 \mu\text{m}$  field of view at a position in the middle of the channel. The morphology represents the surface structure of the spin-coated P3HT layer and

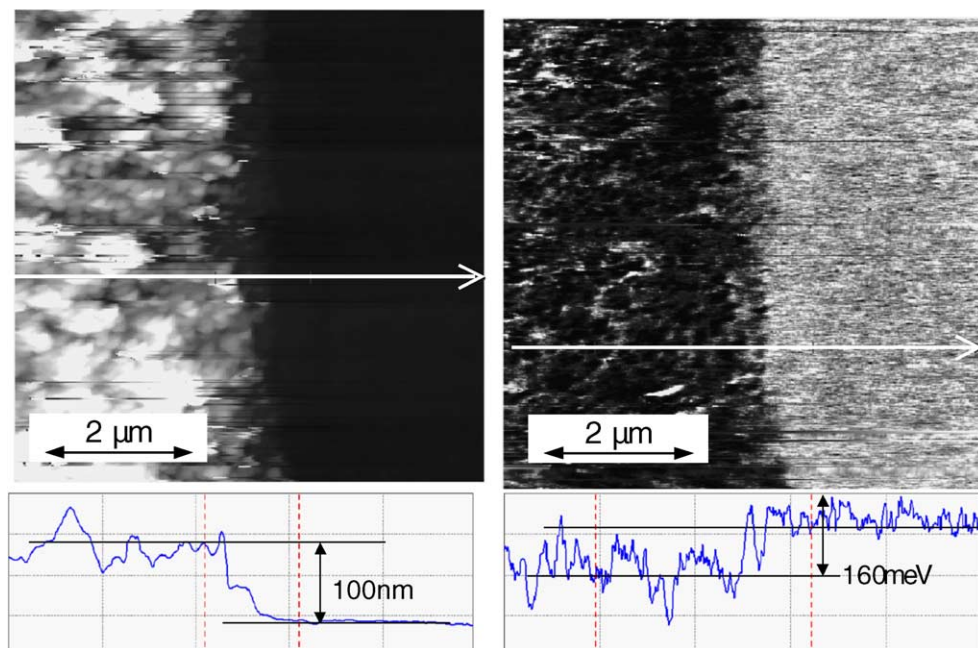


Fig. 4. (A) UHV AFM picture of the P3HT surface at the interface electrode channel. (B) SKPM map with an applied source-drain voltage of +8 V at the same position.

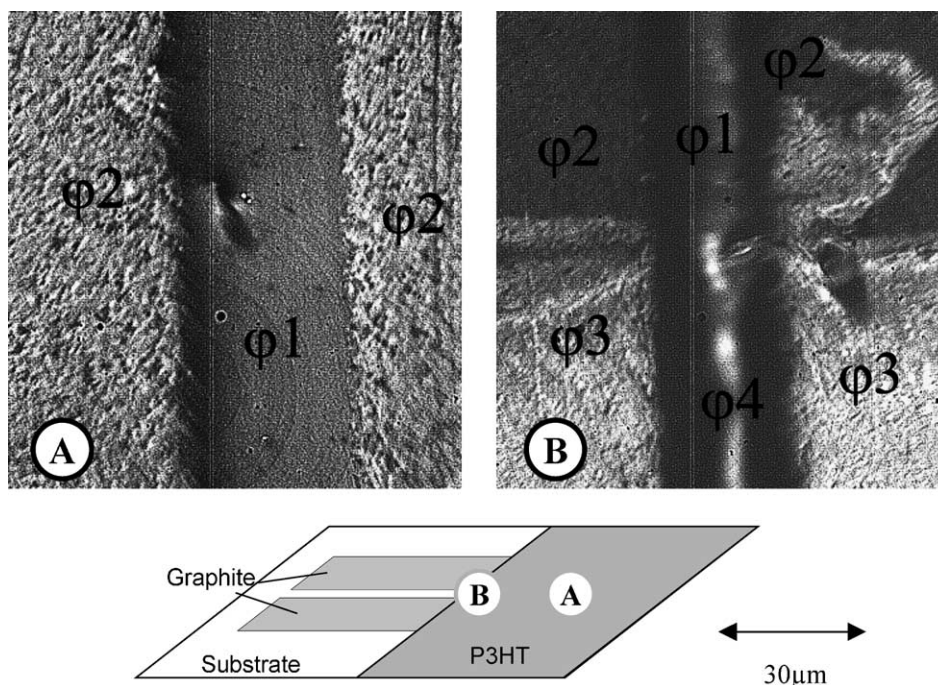


Fig. 5. Hg PEEM images of a source-drain structure made of graphite and spin-coated P3HT. (A) Channel (dark area) and graphite electrodes, covered with P3HT. (B) Channel and graphite electrodes, partially covered with P3HT. The brighter areas represent zones without P3HT and lower surface potentials  $\varphi_i$ , respectively.

shows structures of about 50 nm diameter. Compared to the molecule with a diameter of about 2 nm, such a large diameter indicates agglomerations of P3HT chains.

Fig. 3 demonstrates the spatial resolution of the Kelvin signal contrast compared to the topographic information (Fig. 3A). Fig. 3B shows the two-dimensional electric potential map without any source-drain field applied to demonstrate resolution of measuring the fluctuations of surface potentials. The measured surface potential differences are in the range of around 58 mV in total. Compared to the topographic information, no coincidence of topography and potential distribution was found. This distribution is homogeneous without gradients at large scale. Compared to our SKPM measurements in air, this resolution is much higher and allows characterisation of surface potentials of the semiconductor directly in the channel.

The situation with an applied field of 8 V drain-source is shown in Fig. 3C. The slope of the cut, shown in Fig. 3D, is linear at this position in the channel with a slope value of about 120 mV per  $\mu\text{m}$ . This slope corresponds to the applied voltage in relation to the channel length of 60  $\mu\text{m}$ . Smaller variations of these cuts are due to the above mentioned background of surface potential fluctuations without applied field. Obvious is the further information on the larger scaled variations in the potential in the applied field, resolved clearly in the two-dimensional map (Fig. 3C). This variation is caused by differences in homogeneity of the spin-coated P3HT layer, variations in thickness of the P3HT layer or a variation of the channel length. Consequently this creates an electric field varying along the channel, which is uncovered in Fig. 3C.

After switching the voltage to  $-8$  V drain-source, the distribution of the field is strongly symmetric (reversed).

In Fig. 4A we focus on the interface between the source-drain electrode and the channel. The morphology is displayed in left panel and the potential distribution (with applied voltage of 8 V) in the right panel. For the channel with P3HT a higher workfunction than for carbon black was measured. In SKPM, a potential step of about 160 mV was measured (Fig. 4B), but in contrast to our measurements in air, a smooth onset of the potential in the channel was measured, indicating a good contact between the semiconductor and the carbon black electrode. If we compare the topography and the potential distribution, there is no clear correlation between the features in topography and potential. Also a mismatch between surface structure and local potential is found at the interface electrode/polymer. The contact area in topography is smeared out in a range of 1  $\mu\text{m}$ , but the drop of potential is observed only in a range of 200 nm. Smearing of the contact area is the result of the printing technology, indicating the limit of the used plotting system. Also, the quality of the AFM image in Fig. 4A suffers results from the presence of carbon black particles on the surface. These particles move around, being pushed or pulled by the AFM tip, thus leading to the unstable imaging conditions.

### 3.3. PEEM measurements in UHV

In this section, we demonstrate the principal ability of the PEEM technique to map the lateral morphology, and in addition the distribution of surface potentials with related

chemical composition as a complementary method for the characterisation with SKPM. The PEEM technique is an interesting method, especially for organic materials.

Fig. 5A shows a PEEM image of a surface, prepared with graphite electrodes and P3HT as the upper surface layer. Morphological effects like shadowing gives information about a surface roughness, but the picture is strongly divided into separated areas with different workfunctions:  $\varphi_1$ : P3HT, the channel and  $\varphi_2$ : P3HT + graphite, the electrode. Fig. 5B represents the boundary P3HT as upper layer/pure graphite or substrate. Because the brighter areas represent regions with smaller workfunction (and higher related electron yield rate), we are able to determine the following sequence of workfunctions:  $\varphi_3(\text{graphite}) < \varphi_2(\text{P3HT on graphite}) < \varphi_1(\text{P3HT on substrate}) \approx \varphi_4(\text{substrate})$ . The brighter stripes in the middle of the channel are due to charging effects after 2 h of illumination, caused by the small conductivity of the semiconductor.

In conclusion, PEEM seems to be a new method to give information on the morphology and lateral distribution of workfunctions of organic transistors. Further experiments are performed with applied voltages and in higher resolution in order to develop a complementary method for the SKPM measurements described above.

#### 4. Summary

In this contribution two auxiliary techniques, namely photoemission electron microscopy (PEEM) and scanning Kelvin probe microscopy (SKPM) were utilised to perform a failure mode analysis of OFET source-channel-drain structures. We demonstrate, that SKPM technique is a useful method to characterise the following features of a completely organic transistor structure: (i) the voltage drop at the inter-

face electrode/polymer indicating a contact resistance, (ii) linearity and (iii) local fluctuations of the surface potential due to inhomogenities of the organic layers. In addition, we introduce the PEEM technique as an interesting method to characterise the lateral distributions of the workfunction. By performing UV photoemission we determine the absolute values of the workfunctions of the organic materials used in our source-drain structures.

#### Acknowledgements

The experimental assistance of P. Hoffmann, G. Beuckert and T. Hölzel, as well as the help of the BESSY staff is acknowledged. This work was supported by DFG under grant no. SCHM 745/8.

#### References

- [1] S. Scheinert, G. Paasch, M. Schrödner, H. Roth, S. Sensfuss, T. Doll, *J. Appl. Phys.* 92 (2002) 330–337.
- [2] S. Sadewasser, T. Glatzel, S. Schuler, R. Kaigawa, M.C. Lux-Steiner, *Thin Solid Films* 431 (2003) 257–261.
- [3] L. Bürgi, H. Sirringhaus, R.H. Friend, *Appl. Phys. Lett.* 80 (2002) 2913.
- [4] P. Hoffmann, R.P. Mikalo, D. Schmeißer, *Sol. Energy Mater. Sol. Cells* 72 (1–4) (2002) 517–523.
- [5] P. Hoffmann, R. Mikalo, D. Schmeißer, M. Kittler, *Phys. Status Solidi (b)* 215 (1999) 743.
- [6] P. Hoffmann, Aufbau eines Elektronen-Energie-Analysators ( $\mu$ ESCA) für PEEM, Diploma Thesis, Cottbus (1998).
- [7] K. Müller, I. Paloumpa, D. Schmeißer, *Synth. Met.* 138 (2003) 271–273.
- [8] R. Mikalo, P. Hoffmann, T. Heller, D. Schmeißer, *Solid State Phenomena* 63–64 (1998) 317.